



Cite this: *Environ. Sci.: Atmos.*, 2026, 6, 166

Chemical signatures of water-soluble organic carbon (WSOC) fraction of long-range transported wildfire PM_{2.5} from Canada to the United States Mid-Atlantic region

Esther A. Olonimoyo,^a Martin Changman Ahn,^b Dewansh Rastogi,^b Yue Li,^a Candice M. Duncan^c and Akua Asa-Awuku^{*abd}

Smoke from the Canadian wildfires in the summer of 2023 spread over seventeen million hectares, traveled across the North American continent, and air quality alerts were issued in 20 states in the United States. Its effects were visible in the Northeast and Mid-Atlantic East Coast regions as the air quality index (AQI) increased to very unhealthy levels. For this work, Particulate Matter (PM) samples were collected during the peak of the pollution event in College Park, Maryland, located more than 1000 miles from the source of the fires. Thus, results of this work provide insights into the molecular-level composition of long-range transported wildfire emissions. Specifically, a non-targeted chemical analysis of aerosols collected during and after the wildfire season is presented. The chemical composition of the water-soluble organic carbon (WSOC) compounds is determined using a Bruker Maxis-II Q-TOF mass spectrometer coupled with a Waters Acquity I-Class PLUS LC system. The results reveal a substantial presence of oxyhydrocarbons (CHO) and nitrated oxyhydrocarbons (CHON). Additional compound groups were also detected, incorporating elements such as sulfur, phosphorus, silicon, and various halogens, with chain lengths ranging from C₃ to C₄₁. Our results highlight the prominence of aged water-soluble organic compounds (with O/C ratio ranging from 0.2–0.7) from long-range transported wildfire.

Received 19th September 2025
Accepted 24th November 2025

DOI: 10.1039/d5ea00119f

rsc.li/esatmospheres

Environmental significance

During the 2023 Canadian wildfires, smoke particles traveled over 1000 miles, significantly impacting air quality in urban areas in the United States. Analyzing the chemical composition of these long-range transported particles is essential for understanding their environmental and health implications. This study reveals that oxygenated and nitrated hydrocarbons dominate the water-soluble organic aerosol fraction, providing critical insights into the chemical compounds present in transported wildfire emissions. These findings are crucial for developing strategies to mitigate the adverse effects of widespread pollution events.

1 Introduction

Wildfires are a global phenomenon, and in recent years, they have gained increasing attention due to the impacts of global warming, which has led to more frequent, intense, and prolonged fire seasons on a global scale.^{1–3} According to the Copernicus Atmosphere Monitoring Service, global carbon

emissions from wildfires exceeded 2000 megatons in 2023, marking the highest level recorded in the past two decades.⁴ Additionally, wildfires emit large amounts of toxic gases and particulate matter into the atmosphere and can be transported over long distances across countries and continents, adversely impacting local and regional air quality.^{5,6} Besides altering the atmosphere's chemistry, particulate emissions from wildfires directly interact with the sun's radiation, resulting in haze formation and reduced visibility.⁷ Severe air pollution episodes are experienced in neighboring regions, triggering air quality alerts and health concerns for the exposed populace.⁸

The long-range transport of wildfire emissions is driven by plume height, fuel load, and meteorological conditions. The transport *via* space and time results in air mass aging and chemical modification, forming new complex compounds through chemical reactions with atmospheric oxidants (*e.g.*, but not limited to hydroxyl and nitrate radicals), thus significantly

^aDepartment of Chemistry and Biochemistry, University of Maryland, College Park 4418 Stadium Drive, Building (090), College Park, MD 20742, USA. E-mail: estherao@umd.edu; yueli@umd.edu; asaawuku@umd.edu

^bDepartment of Chemical and Biomolecular Engineering, A. James Clark School of Engineering, University of Maryland, College Park, College Park, MD 20742, USA. E-mail: mahn@umd.edu; drastogi@umd.edu

^cDepartment of Environmental Science and Technology, University of Maryland, College Park, College Park, MD 20742, USA. E-mail: cduncan1@umd.edu

^dDepartment of Civil and Environmental Engineering, University of Maryland, College Park, College Park, MD 20742, USA



impacting atmospheric particle chemistry.⁹ Depending on their sizes, these emitted particles can persist in the atmosphere from weeks to months.¹⁰ Studies have examined long-range transported wildfire emissions from aircraft, satellite observations, and modeling studies, but fewer have investigated wildfire emissions from a ground-based observation.¹¹ There is a noticeable knowledge gap in the chemical composition of ground-based observations of long-range transported air masses, making such observations essential for a more comprehensive understanding of their effects on human exposure and regional air quality.

The chemical composition of emitted smoke particles depends on several factors, including fuel type and volume, soil type, the degree of combustion, and combustion conditions such as moisture content and temperature.^{7,12,13} The organic composition of PM_{2.5} emitted from wildfires is complex and can make up more than 90% of the total aerosol composition;¹⁴ however, few studies have characterized the elemental and molecular-level composition of smoke that has undergone long-range transport. Furthermore, within this broad spectrum of compounds, water-soluble compounds are of particular interest because they are easily oxidized and contribute to aqueous phase atmospheric reactions. Water-soluble compounds also interact with water vapor to reduce visibility, form cloud condensation nuclei, influence cloud properties, and indirectly affect the earth's radiation balance.^{15,16}

In characterization studies of atmospheric particles, several techniques can be classified as offline, online, or *in situ*.^{17–21} While offline methods involve separate particulate sampling and extraction steps followed by chemical speciation, online and *in situ* modes enable a continuous sampling measurement, reducing sample handling and allowing for real-time or near real-time characterization.^{21,22} Traditionally, gas chromatography (GC) and liquid chromatography (LC) techniques have been coupled with mass spectrometry (MS) for chemical speciation of atmospheric particulate matter.²³ While GC is more suitable for volatile compounds such as volatile organic compounds (VOCs) and polycyclic aromatic hydrocarbons (PAHs), LC is better suited for less volatile compounds such as polar organic acids and high-molecular-weight oxygenated compounds.²⁴ The use of mass spectrometers provides high sensitivity and selectivity in data outputs.²⁵ More recently, there has been a rise in the use of aerosol mass spectrometers (AMS), which effectively offer real-time size-resolved chemical speciation data.^{26,27}

Several targeted analyses focusing on specific chemical species have been reported in the literature. For instance, LC-MS (Q-TOF) has been applied to characterize amino acids in aerosols from a Southern U.S. Forest,²⁸ and Q-TOF was similarly used to investigate organosulfates in atmospheric aerosols across the Asian region.²⁹ Seasonal and diurnal variations of particulate organosulfates in urban Shanghai were also examined using targeted methods.³⁰ To obtain a more comprehensive chemical speciation profile, non-targeted approaches have increasingly been employed. In China, airborne microplastics and additives were analyzed on an LC-MS/MS platform using a non-targeted strategy.³¹ Likewise, a non-targeted molecular-

level study of organic aerosols in Beijing revealed a high degree of oxidation, with notable contributions from organosulfates and nitroaromatic compounds.³² In addition, a GC-QTOF/MS system was employed in a non-targeted investigation of persistent organic pollutants collected with passive air samplers in Toronto.³³

In this work, we characterize water-soluble organic compounds in particulate matter sampled in the Mid-Atlantic region on the East Coast of the United States, in the urban area of College Park, Maryland. The fire activity from Canadian wildfires in 2023 was more intense than previous decades and carbon emissions from wildfires rivaled that of the top ten largest emitting countries.^{34,35} The air pollution event that occurred during the summer of 2023 provides a unique opportunity to study the influence of long-range transported wildfire smoke on the East Coast of the United States. Additionally, we compare aerosol chemical composition during the pollution episode influenced by Canadian wildfires to regional air measured months after. We also explore diurnal changes in the water-soluble organic fraction of wildfire plumes with aging. The results have implications for our understanding of wildfire emissions across urban centers, climate, air quality, and health.

2 Methods

2.1 Study area

Wildfires in Canada were reported in May 2023 (ref. 36) and intensified in June 2023.^{35,37} The air pollutants noticeably affected over 160 million people on the North American East Coast (Fig. 1). About 20 U.S. states experienced severe air pollution, triggering air quality alerts and reduced visibility. Although wildfires are year-round and intercontinental, we hereby refer to this particular event in as the East Coast Canadian Wildfire event. The pollutant effects were visible in College Park, Maryland, as the air quality index (AQI) increased to very unhealthy levels (AQI > ~100). In the AQI chart, values ranging from 0 to 50 indicate good air quality, while those between 51 and 100 represent moderate conditions. AQI values above 100 are considered unhealthy: 101 to 150 are classified as unhealthy for sensitive groups, 151 to 200 as unhealthy for the general population, 201 to 300 as very unhealthy, and 301 to 500 as hazardous.

Air particles were sampled actively from the rooftop lab of the Atmospheric and Oceanic Sciences building (~15 m a.g.l.), located on the University of Maryland campus at College Park (GPS coordinates: 38.99, -76.94). College Park, Maryland, is roughly 6 miles from the US capital, Washington D.C., and is located in a populous urban metropolitan center. Additional data was acquired from the Maryland Department of the Environment (MDE) operated U.S. Environmental Protection Agency (EPA) air quality monitoring station located in Beltsville, Maryland, 5 miles from the College Park particle sampling site (GPS coordinates: 39.06, -76.88). The Beltsville collection site is part of the EPA's Ambient Air Monitoring Network (AMTIC) and provides information for the Chemical Speciation Network (CSN).



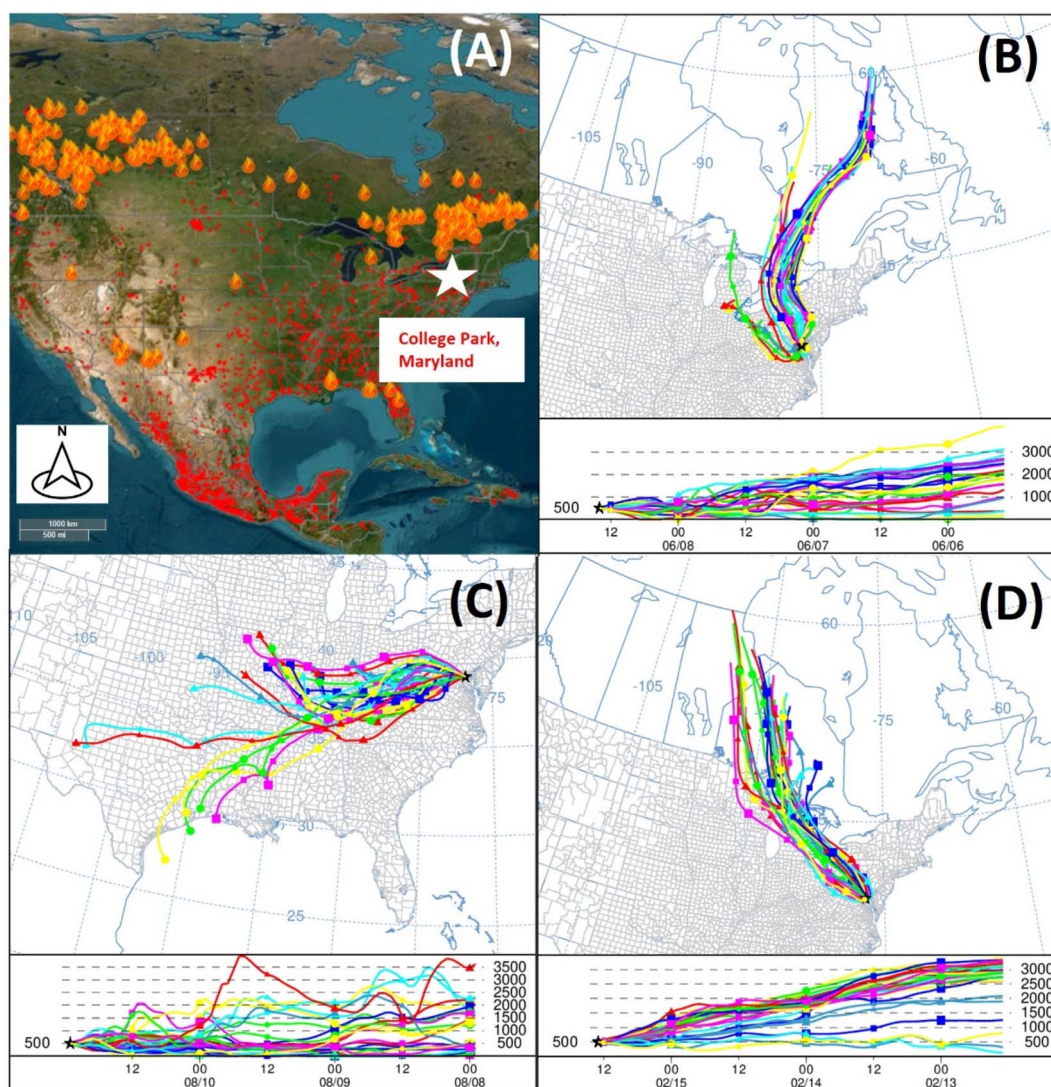


Fig. 1 (A) Location of wildfires in North America in June 2023. While the flame icons represent active wildfire activity, the red dots represent satellite detected fire activity which may include agricultural bush burning etc. (image source: adapted from NASA Fire Information for Resource Management System (FIRMS) US/Canada (<https://firms.modaps.eosdis.nasa.gov/usfs/map/>), 2023) and HYSPLIT back trajectories showing air masses that traveled south from the wildfires during the wildfire season – WF-N1 (B), and back trajectories of air masses post-wildfire in August 2023 – PF-2M-D and February 2024 – PF-8M-N, respectively (C and D).

2.2 Particulate sampling and extraction

Air particles were sampled at a flow rate of 29 L min^{-1} onto a $0.22 \mu\text{m}$ polyvinylidene fluoride (PVDF) membrane filter (Millipore Sigma, Burlington, MA). During the East Coast Canadian Wildfire event, samples were collected from June 7th to June 9th, 2023, during the day (9 am to 6 pm EST) and at night (6 pm to 9 am EST) (Table 1). Henceforth, samples collected during the day and night are denoted by the letters D and N, respectively (e.g., wildfire samples collected during the day and night are referred to as WF-D and WF-N, respectively). Continuous particulate sampling was also performed for a 60 hour period (2.5 days) from June 9th to June 12th, 2023. The sample collected during this time is referred to as WF-2.5.

In August of the same year, 2 months later, there was no visible evidence of smoke in the region, and the AQI on the sampled day showed good air quality (AQI < 100, Table 1). Post-wildfire daytime

and nighttime samples were collected from August 9th–10th (PW-2M-D and PW-2M-N) and February 15th–16th (PW-8M-D and PW-8M-N). All collected membranes were extracted in 20 mL of ultra-purified water ($18.2 \text{ M}\Omega \text{ cm}$, ELGA Purelab Option-Q unit) by sonication and heating ($40 \text{ }^\circ\text{C}$) for 1 hour, filtered (90 mm filter paper, Grade 1: $11 \mu\text{m}$ Whatman), and refrigerated until chemical analysis.³⁸ Sample, instrument, and method blanks were also included in the LC/MS-MS analysis. All data presented subtract contributions from blanks and are the average of triplicate measurements. A total of nine samples were collected, including five wildfire samples and four post-wildfire samples.

2.3 Liquid chromatography-tandem mass spectroscopy (LC/MS-MS) and data analysis

Chemical analysis was performed with a Waters Acquity I-Class PLUS Liquid Chromatography system (Waters Corporation, MA,



Table 1 Description of collected aerosol samples and sampling conditions

	Dates	Period	Sample time		Sample name	AQI ozone ^a	AQI PM _{2.5} ^a
			Eastern standard (UTC-05:00)	UTC		[#, ppbv]	[#, µg m ⁻³]
Wildfire (WF) season	June 7th–8th, 2023	Nighttime	6 pm to 9 am	11:00 to 13:00	WF-N1	80, 64	157, 66.8
		Daytime	9 am to 6 pm	13:00 to 23:00	WF-D1	74, 62	181, 114.2
	June 8th–9th, 2023	Nighttime	6 pm to 9 am	11:00 to 13:00	WF-N2	40, 43	62, 17.3
		Daytime	9 am to 6 pm	13:00 to 23:00	WF-D2	50, 54	50, 11.9
Post-wildfire 2 months (PF-2M)	June 9th–12th, 2023	2.5 days	6 pm to 9 am	11:00 to 13:00	WF-2.5	67, 58 ^b	51, 13.7 ^c
	August 9th–10th, 2023	Nighttime	6 pm to 9 am	11:00 to 13:00	PF-2M-N	49, 53	38, 9
Post-wildfire 8 months (PF-8M)	February 15th–16th, 2024	Daytime	9 am to 6 pm	13:00 to 23:00	PF-2M-D	34, 37	41, 9.8
		Nighttime	6 pm to 9 am	11:00 to 13:00	PF-8M-N	31, 34	2, 0.5
		Daytime	9 am to 6 pm	13:00 to 23:00	PF-8M-D	36, 39	3, 0.6

^a Daily AQI values were obtained for ozone and PM_{2.5} from the site (HU-Beltsville), ID (240330030), Agency (Maryland Department of the Environment). ^b WF-2.5, AQI ozone = 87 and 46 for day 1 and 2, respectively; the average is reported in the table. AQI ozone concentration was 66 and 50 ppbv, for day 1 and day 2, respectively; the average is reported in the table. ^c WF-2.5, AQI PM_{2.5} = 64 and 38 for day 1 and 2, respectively; the average is reported in the table. AQI PM_{2.5} concentration was 18.3 and 9.1 µg m⁻³ for day 1 and day 2, respectively; the average is reported in the table.

USA) coupled to a Bruker Maxis-II, ultra-high resolution Q-TOF mass spectrometer using electrospray ionization (ESI). Chromatographic separations were performed with an Acquity UPLC BEH C18 Column, 130 Å, (1.7 µm, 2.1 mm × 100 mm, Waters Corporation, MA, USA) with 0.1% formic acid (LC-MS Grade, Fisher Scientific) in ultra-pure water (18.2 MΩ cm, ELGA Purelab Option-Q unit) and 0.1% formic acid in acetonitrile (LC-MS Grade, Fisher Scientific) as mobile phase solutions A and B, respectively for a total run time of 25 minutes. At a flow rate of 0.25 mL min⁻¹ and injection volume of 5 µL, initial conditions were set at 95% A in the first 14 minutes, then changed linearly to 40% for 6 minutes and returned to 95% for 5 minutes. The column temperature was operated at 30 °C.

The Bruker Maxis-II Q-TOF mass spectrometer (resolving power: 80 000) was operated under the following settings: capillary voltage = 4500 V, endplate offset voltage = 500 V, dry gas flow rate = 5.0 L min⁻¹, and the ion source temperature = 220 °C. The mass spectrometer was operated in positive and negative modes, scanning across 80 to 800 and 50 to 600 *m/z* mass ranges, respectively. In mass spectrometry, analyte detection relies on the ionization of compounds, which enables their conversion into charged species. Depending on their chemical structure and functional groups, compounds can ionize either positively or negatively, resulting in data acquisition in positive or negative ionization modes. Additionally, compounds may ionize to varying degrees, influencing their detection sensitivity and signal intensity. The experimental data were acquired using the Bruker Q-TOF Control and Compass Hystar software (version 5.1, Bruker) and analysis was completed using the Compass Metaboscape software (version 5.0, Bruker).

A Principal Components Analysis (PCA) technique was used as an unsupervised method for data visualization and outlier identification. The *t*-test calculated the *p*-value and fold change (FC). All the ion peaks with *p*-value < 0.05 and FC > 0 were highlighted as the differential ions. Those ions were tentatively identified based on accurate mass measurements and MS/MS

spectral matching using the Natural Products Atlas database, the National Institute of Standards and Technology (NIST) MS/MS library (2020), and the MassBank of North America (MoNA) library. The oxygen to carbon (O : C) elemental ratio can be determined from chemical speciation data. Here, we report the bulk O : C ratio of the water-soluble organic composition as the weighted average of each identified compound's O : C scaled by its relative peak intensity. O : C values are calculated using the I-A method by Canagaratna *et al.*, 2015, and details are provided in the SI.³⁹

2.4 Hybrid Single-Particle Lagrangian Integrated Trajectory (HYSPLIT) analysis

Air mass backward trajectories were performed on the web version of the Hybrid Single-Particle Lagrangian Integrated Trajectory (HYSPLIT) model (Fig. 1B–D and S1). The HYSPLIT model from the National Oceanic and Atmospheric Administration (NOAA), which combines a Lagrangian and Eulerian approach, simulates the transport of air masses.⁴⁰ A 72 hour backward trajectory was computed using the 1° Global Data Assimilation System (GDAS) for each sample collected. The analysis provides insight into the source and direction of pollutants observed in the region.

3 Results and discussion

3.1 Back trajectory analysis

According to the Canadian 2023 fire season report from the Canadian Interagency Forest Fire Centre Inc. (CIFFC), about 17 million hectares were burned in Canada during the 2023 wildfire season.⁴ The burned areas consisted of boreal forests, mixed forests, and coastal rainforests and were composed of various vegetation species such as black spruce, white spruce, and balsam fir.⁴¹ Meteorological conditions such as wind speed and direction, temperature, and relative humidity aided the spread and transport of smoke and particulate emissions.



HYSPLIT modeling results confirm that the wildfire air mass traveled approximately 1000 miles across several urban centers, including but not limited to Ottawa, Toronto, Quebec, Montreal, Pittsburgh, Philadelphia, New York City, and Washington DC (Fig. 1B). Fig. 1B shows that the air mass sampled in College Park, MD, was aged in the atmosphere for roughly 2–3 days. During transport, the air mass sampled at College Park stayed within the tropospheric boundary layer. Each trajectory (Fig. 1B–D) shows the composition was well-mixed vertically within the tropospheric boundary layer. Back trajectories provide evidence that the WF samples are influenced by Canadian wildfire emissions.

3.2 Organic chemical composition – water-soluble organic compounds

Peak areas were used for relative quantification within each positive and negative ionization mode. Due to differences in ionization efficiency and total signal response between modes, percent relative compositions were calculated and reported separately for each ionization mode and compound group. A total of 316 unique ions were detected, comprising 59 and 257 unique organic compounds identified in positive and negative ionization modes, respectively. These values represent the number distributions of ions identified and discussed in this work. These compounds were classified into 11 groups based on their elemental composition. CHO and CHON ions constituted the majority of reported compounds, with 194 and 51 ions in both positive and negative modes, respectively, accounting for over 75% of the WSOC ions in wildfire samples in both ionization modes (Table 2). Carbon, hydrogen, oxygen, and nitrogen are the most common elements identified in the wildfire season samples, consistent with speciation from previous biomass sampling studies.^{10,42} Other elements, such as sulphur, phosphorus, halides (fluorine, chlorine, and bromine), and silicon, were found in fewer ions (<25%, Table 2).

The most dominant compound group is oxy-hydrocarbons (CHO), with 32 and 162 ions detected in positive and negative modes, respectively. The most common ions within the CHO group in positive mode included C₅H₆O₂, C₆H₁₂O₂, C₃₈H₆₂O₉,

and C₈H₈O₅, while in negative mode, C₄H₂O₄, C₆H₁₂O₆, C₁₅H₂₂O₄, and C₂₀H₂₄O₂ were prevalent. In the CHON group, 15 ions were identified in positive mode, and 36 in negative mode. The most abundant ions in this group were C₅H₉NO, C₃₀H₄₆N₆O₆, C₂₀H₁₄N₄O₃, C₅H₄N₄O, and C₁₂H₁₅NO₄. Throughout the sampling week, the presence of these groups did not show significant changes within the first 48 hours, indicating no notable diurnal variation (Fig. 2). Several compounds were detected with identical molecular formulas and *m/z* values but different retention times, indicating the presence of isomeric species. For example, two features assigned to C₈H₁₂O₃ (*m/z* –157.08) were separated at retention times of 6.71 and 8.77 minutes, supporting the existence of structural isomers.

Other nitrogen-containing WSOCs included the CHONP class, representing organics containing both nitrogen and phosphorus. A total of six CHONP species were identified across both ionization modes, with C₁₅H₂₄N₂O₁₇P₂ and C₃₄H₆₆NO₉P contributing the most to the overall abundance. Although rare, CHONP compounds have previously been reported in wildfire smoke, where they accounted for less than 6.5% of the identified molecular formulas.⁴³ The CHONS class comprised 11 ions, detected exclusively in the negative mode. Among these, C₁₉H₂₀N₂O₇S and C₂₇H₃₉N₂O₅S showed the highest relative abundance. While detected in smaller amounts, CHONS compounds have been highlighted in previous studies and are thought to arise primarily from biogenic precursors, subsequently forming through secondary processes in the atmosphere.^{29,44} Additionally, CHN compounds were identified exclusively in the positive mode, totaling five ions, with C₇H₁₀N₂ and C₂₁H₂₈N₂ being most prominent. Literature reports associate CHN compounds with alkaloids, naturally occurring nitrogenous organics released during the pyrolysis of biomass and detected in long-range transported WSOC.^{45–47}

The CHOP class was dominated by C₄₁H₇₃O₇P and C₃H₉O₆P, which contributed most strongly to this group. CHOPs, commonly referred to in literature as organophosphates, are recognized as emerging pollutants due to their potential toxicity. They have been reported as products of the combustion

Table 2 Elemental classification of wildfire season samples

Compound groups	Formula	Number of ESI signals/ions	
		Positive mode	Negative mode
Nitrate-oxy hydrocarbons	CHON	15	36
Oxy-hydrocarbons	CHO	32	162
Phosphorus nitro-oxy hydrocarbons	CHONP	2	4
Nitrated hydrocarbons	CHN	5	—
Silicon-oxy hydrocarbons	CHOSi	1	—
Hydrocarbons	CH	1	—
Phosphorus-oxy hydrocarbons	CHOP	1	17
Sulphur-oxy hydrocarbons	CHOS	1	11
Sulphated hydrocarbons	CHS	1	—
Halogenated hydrocarbons ^a	CHX	—	16
Nitro-oxy-sulphur hydrocarbons	CHONS	—	11

^a In halogenated compounds; X = fluorine, chlorine, bromine.



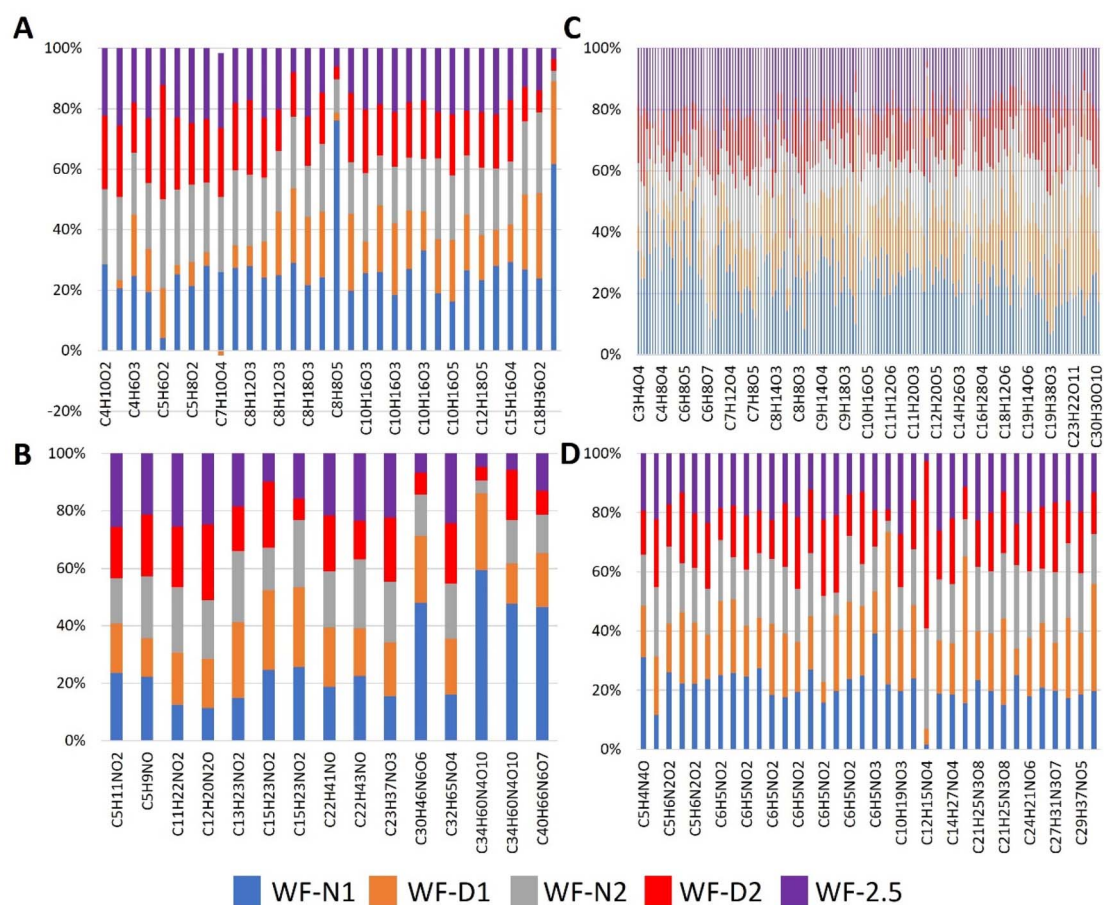


Fig. 2 Percentage abundance of uniquely identified compounds observed during the wildfire (WF) sampling season: (A) positive mode, CHO, (B) positive mode, CHON, (C) negative mode, CHO, (D) negative mode, CHON. This figure shows a comparison of samples WF-N1 (blue), WF-D1 (orange), WF-N2 (grey), WF-D2 (red), and WF-2.5 (purple) across increasing carbon chain length (x-axis, left to right).

of phosphorus-rich vegetation as well as from the burning of plastics and other synthetic materials.^{48–50} Other sulfur-containing species included the CHOS class, which comprised 12 distinct ions across both ionization modes. Among these, $C_{14}H_{18}O_5S$ and $C_5H_8O_3S$ contributed the highest abundances. CHOS species reported in the literature are frequently associated with isoprene oxidation products, pointing to important roles for both primary emissions and secondary atmospheric processing.²⁹ In addition, halogenated hydrocarbons were detected in the CHX class, with a total of 16 compounds observed. The most abundant included $C_{10}H_{10}Cl_2$ and $C_{30}H_{27}ClO_7$. Similar halogenated structures, such as chlorinated polycyclic aromatic hydrocarbons (Cl-PAHs), have been identified from the combustion of coal.^{51,52} While combustion remains the dominant source, a study conducted in Hong Kong suggested that halogenated hydrocarbons may also arise in negligible amounts from biomass and biofuel burning.⁵³

Other minor groups were also observed, including CH, CHOSi, and CHS, each represented by a single compound. Although present at lower abundance, the detection of CHOSi and CHS compounds further reflects the diversity of heteroatom-containing organic compounds present in combustion-derived WSOC. Across all compound groups, no

pronounced sample-to-sample variability was observed in the wildfire dataset, with abundances remaining relatively stable throughout the sampling week.

The length of the carbon chain makes up the core structure of organic compounds and significantly influences their inherent physicochemical properties. In this study, the observed chain lengths ranged from C_3 to C_{41} in positive mode and C_3 to C_{32} in negative mode, consistent with previous reports of diverse chain-length distributions in atmospheric organic aerosols.³¹ Shorter-chain compounds (C_1 – C_5) are generally more volatile and water-soluble, which facilitates their participation in faster atmospheric reactions and removal by wet deposition. Conversely, longer-chain compounds ($>C_{10}$) are less volatile and more hydrophobic at emission, but when exposed to oxidative processes, they can undergo fragmentation, producing shorter-chain dicarboxylic acids and related oxygenated species (Fig. 3).

This process is important during long-range atmospheric transport, where progressive aging converts primary emissions into smaller, highly oxygenated, water-soluble products such as oxalic acid.^{54,55} In the WSOC ions described in this study, approximately 50% were longer chains in the positive mode, while about 43% were longer chains in the negative mode. This



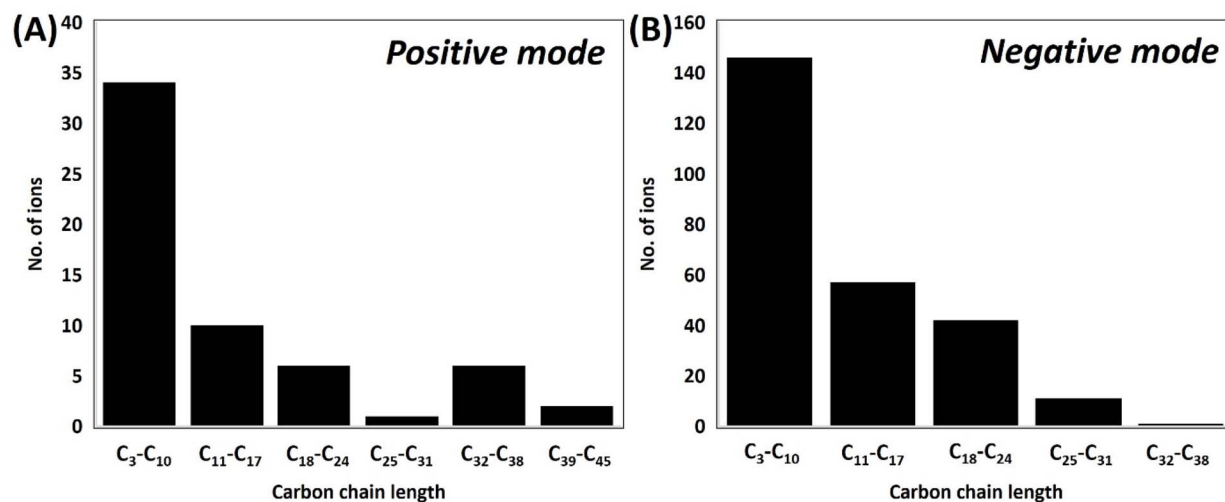


Fig. 3 Distribution of carbon chain lengths of measured ions reported during the wildfire (WF) sampling period in (A) positive mode and (B) negative mode. More ions were detected in the negative mode than in the positive mode because most water-soluble extracted compounds are polar and ionize better in negative mode.

observation highlights the carbon chain length distribution of WSOCs in aged aerosols from wildfire smoke.

Observed O : C values ranged between 0.23 and 0.26 with an average of 0.25 in the positive mode and 0.59 and 0.70 with an average of 0.62 in the negative mode (Fig. 4). O : C values in the positive mode tend to be lower as they account for less oxygenated compounds. Our values in the negative mode fell within the range reported by Brito *et al.*, 2014.⁵⁶ They studied aerosols observed at ground level significantly influenced by regional Biomass Burning (BB) plumes while Zhou *et al.*, reported higher values for aerosols in BB plumes (0.69) and influenced by BB (0.77). Their report represents observations from an elevated observatory (the Mount Bachelor's Observatory) studying the regional influence of wildfires.⁵⁷

Higher O : C values indicate more oxidation, mixing and aging processes. Although⁵⁸ reported a lower O : C average value (0.42) for biogenic aerosols, their observation was not linked to

a BB but was interpreted to represent secondary organic aerosols (SOA). Lower values (0.22 and 0.33) were also reported for biomass burning organic aerosols (BBOA).^{27,59} In both studies, observations were made from urban ground-level sites. Our observations show a degree of aging and oxidation undergone by the long-range transported wildfire emissions and the presence of SOA formation.

3.3 Aging and long-range transport

Most of the water-soluble chemical composition PM remained constant over the wildfire season samples. The relative amount of the most abundant compound groups (CHO and CHON) remained constant in the wildfire season samples (Fig. 2). The AQI (PM_{2.5}) in College Park dropped from 181 (unhealthy) to 62 (moderate) between the 8th and 9th of June (Table 1). Although the air quality indices improved significantly within the wildfire sampling season, the peak abundance remained constant for each compound group. Thus, changes in AQI and a reduction in total PM mass loading are not necessarily reflective of changes in atmospheric particle chemical composition.

Surprisingly, the same trend is also observed for night and day samples. Nighttime samples are likely to have an increased composition of nitrogen-containing compounds due to their reactions with nighttime radicals (NO₂ and NO₃). Fig. 2 also shows little to no variance in the change in WSOC elemental composition between the nighttime and daytime wildfire season samples. This suggests that diurnal variation (nighttime *versus* daytime reactions) far from the source had little to no effect on the water-soluble organic chemical composition of the collected samples. Upon injection into the atmosphere, wildfire emissions undergo chemical (photochemical reactions (with light) and other chemical constituents (ozone, hydroxyl radicals)) and physical processes (*e.g.*, dry deposition, wet scavenging, and precipitation). The measurements obtained at College Park, MD, suggest the air mass at this location has

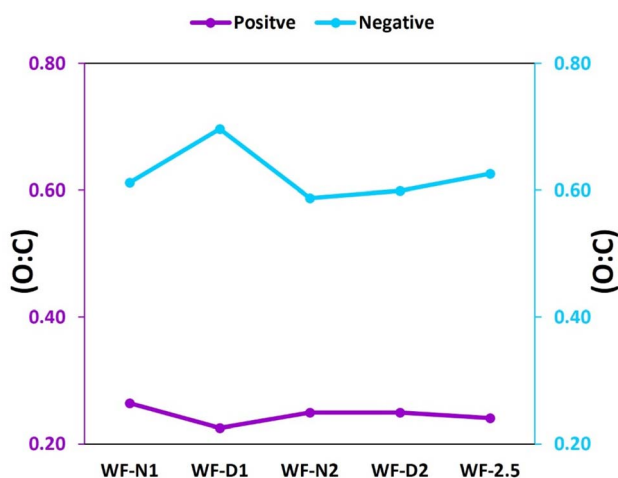


Fig. 4 O : C ratio of prevalent WSOC compounds reported during the wildfire (WF) sampling period.



already gone through a continuous sequence of reactions, and the water-soluble organic chemical concentrations have reached pseudo-steady-state values and transported more than 1000 miles may change little over the course of 2–3 days.

3.4 Post-wildfire measurements

3.4.1 Background period: 8 months post-wildfire. The samples collected during the 8 month post-wildfire sampling event were considered to be representative of background air

quality for the region and are hereon referred to as the background. Although, back trajectories show that sampled air mass at this time came from the direction of the Canadian wildfire region, samples collected 8 months after the wildfire event (PF-8M) have a considerably different composition than the water-soluble organic species identified during the wildfire season (Fig. 1D). The AQI for PM_{2.5} and ozone during observations (Table 1) were low and green (indicating good air quality). By this sampling time, seasonal changes have occurred (from

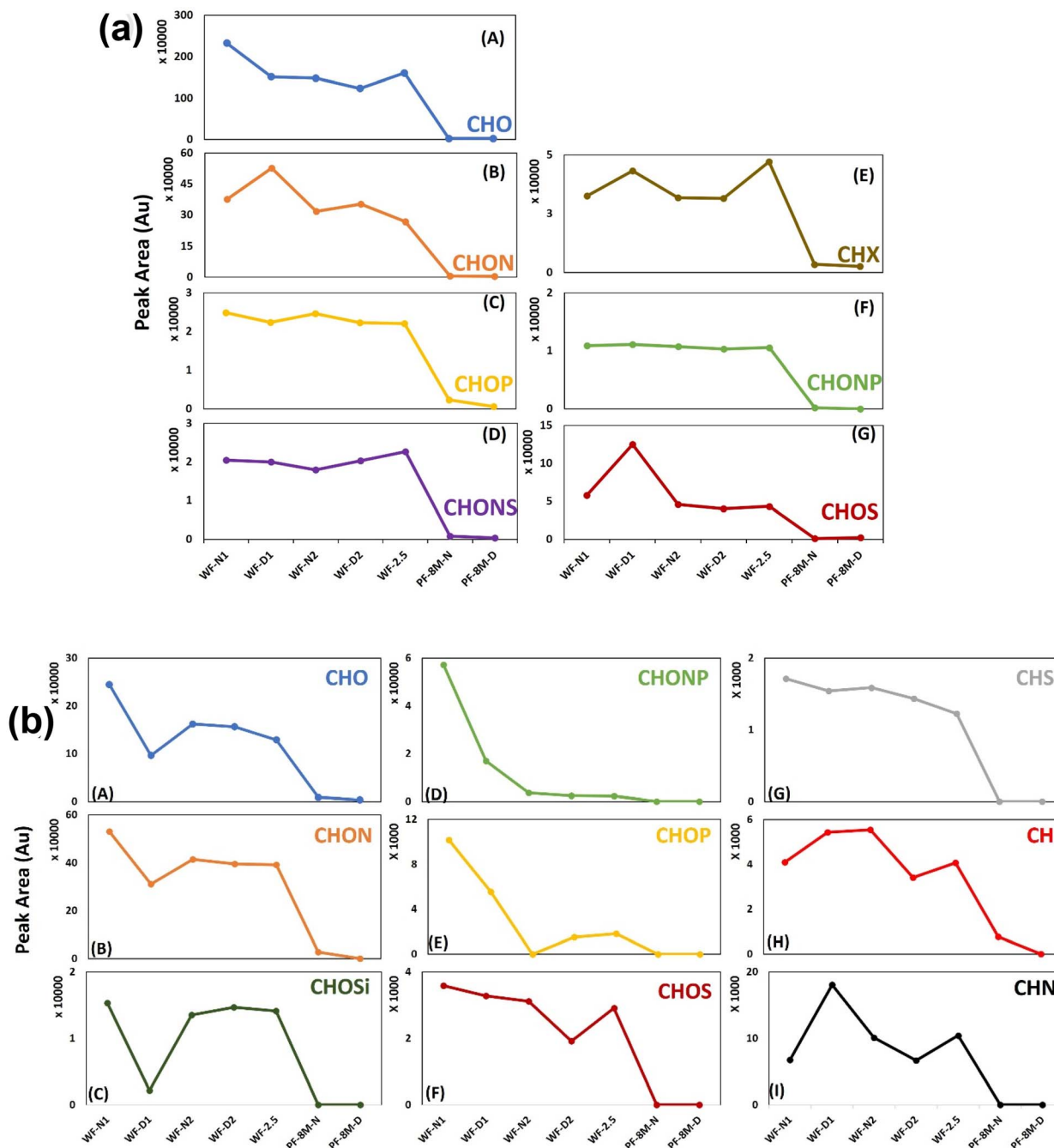


Fig. 5 (a) Relative abundances of compound groups detected in negative mode during wildfire (WF) and eight months post-wildfire (PF-8M) sampling seasons: (A) CHO, (B) CHON, (C) CHOP, (D) CHONS, (E) CHX, (F) CHONP, (G) CHOS. (b) Relative abundances of compound groups detected in positive mode during wildfire (WF) and eight months post-wildfire (PF-8M) sampling seasons: (A) CHO, (B) CHON, (C) CHOSi, (D) CHONP, (E) CHOP, (F) CHOS, (G) CHS, (H) CH, and (I) CHN.



summer to winter), and several precipitation events, allowing for both dry and wet deposition processes to remove atmospheric pollutants, have occurred. Fig. 5a and b also shows that the absolute abundance of all the reported compounds in the wildfire samples is significantly lower in the background samples.

Although the differences are subtle, variations between the nighttime and daytime samples of the 8 month post-wildfire samples are observed. The PF-8M-N samples contain more

CHON and CHONP compounds, consistent with the expected contributions of PM nighttime radical chemistry.⁶⁰

3.4.2 Influence period: 2 months post-wildfire. Additional samples were acquired in August 2023 (nine weeks after the wildfire event), when there was no visible indication of air pollution from wildfires as in the wildfire season in July. The AQI levels for both ozone and PM in August were lower than during the wildfire event, and regional visibility was significantly improved (Table 1). However, results show the presence

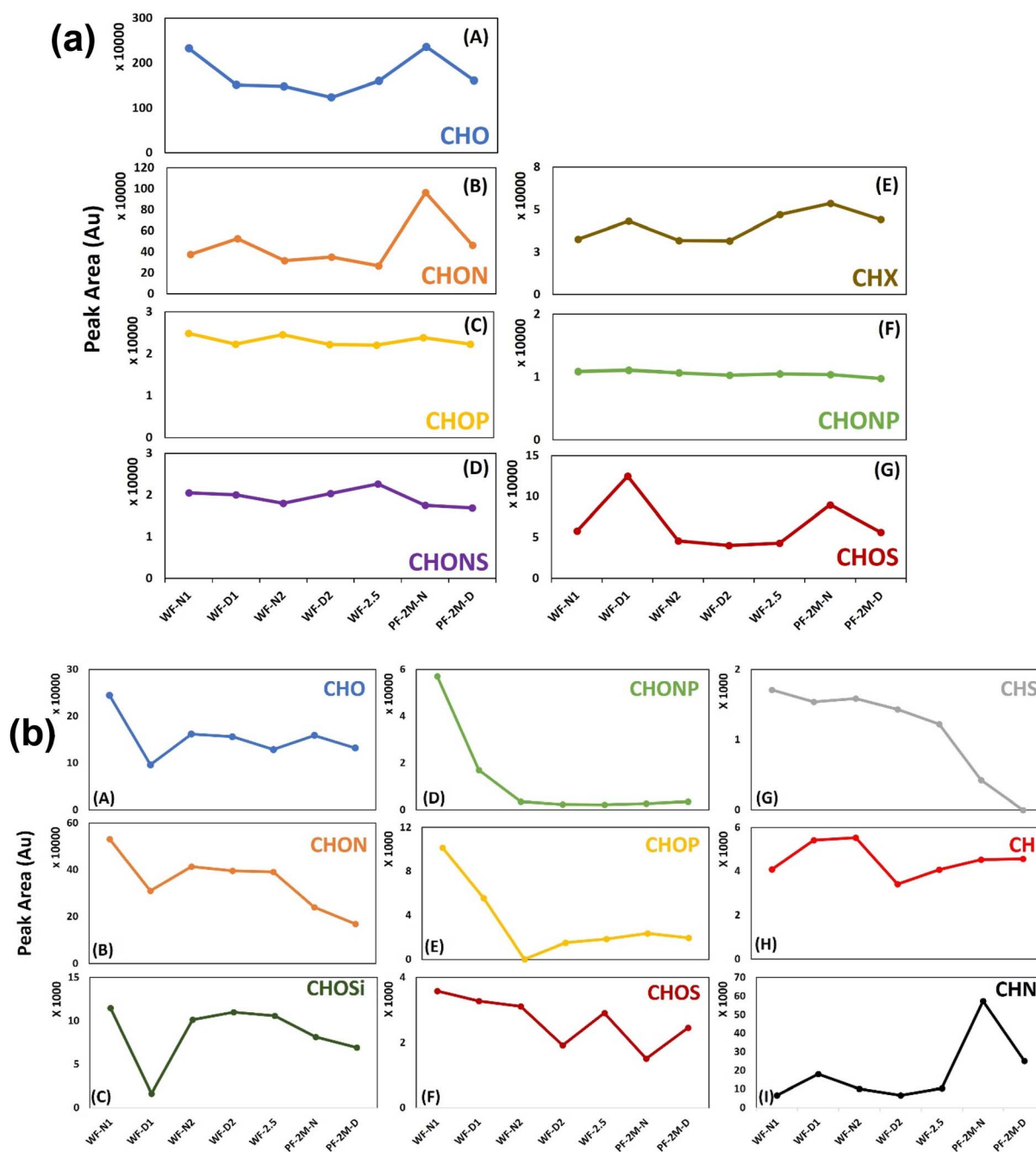


Fig. 6 (a) Relative abundances of compound groups detected in negative mode during wildfire (WF) and two months post-wildfire (PF-2M) sampling seasons: (A) CHO, (B) CHON, (C) CHOP, (D) CHONS, (E) CHX, (F) CHONP, (G) CHOS. (b) Relative abundances of compound groups detected in positive mode during wildfire (WF) and two months post-wildfire (PF-2M) sampling seasons: (A) CHO, (B) CHON, (C) CHOSi, (D) CHONP, (E) CHOP, (F) CHOS, (G) CHS, (H) CH, and (I) CHN.



of persistent WSOC compounds, similar to those observed in wildfire samples (Fig. 6a and b). We consider this an “influence period” describing samples collected in College Park, MD when there was no visibly evident air pollution, yet, chemical analysis of WSOC indicates similar compounds are identified in sampled PM.

It should be noted that active wildfires were recorded in Canada and the western U.S. during this active sampling period but at a lower intensity compared to the East Coast-Canadian Wildfire event and in a different location. Obtained HYSPLIT images confirmed that air masses did not travel from intense fire-active regions and the 48 hour long-range air mass in College Park, MD likely originated from South Dakota, Nebraska, Iowa, Illinois, Michigan, and Indiana (Fig. 1C). This observation suggests that chemical signatures from long-range transported wildfire emissions can persist in a region longer than air quality indices can tell us. This finding is consistent with the work of Lee *et al.*, 2022, who found that 49% of the cloud water sampled at White Face Mountain was influenced by transported wildfire smoke from Canada.⁶¹ Ultrafine particles ($PM_{1.0}$ and $PM_{2.5}$) remain suspended in the atmosphere for prolonged periods, modifying their chemistry. The degree of rain events, wind speed, direction, and temperature are other meteorological conditions may contribute to the atmospheric removal of organics after wildfire events.

3.5 Levoglucosan and other noteworthy compounds

Data obtained from the Beltsville Monitoring site and EPA Chemical Speciation Network (CSN) is shown in Fig. 5. Although obtained separately at a location different from the College Park sampling site, the data shows significant aerosol burden (up to $120 \mu\text{g m}^{-3}$) in the region during the 2023 Canadian wildfire event. Fig. 7 also shows that the potassium ion (K^+), an indication of biomass burning emissions, was also measured.^{10,62}

Our observations indicate significant spikes (up to 4–6 times higher) in $PM_{2.5}$ and K^+ during the peak of the event which was also the same time samples were obtained in College Park. During the sampling period, organic carbon (OC) was twenty times higher than elemental carbon (EC) thus indicating that semi-volatile organic carbon species was a significant contribution to the carbonaceous aerosol contribution. The data from CSN also show that two months post-wildfire, the levels of $PM_{2.5}$ and K^+ were significantly lower than that measured during the wildfire event.

A comprehensive list of detected WSOC compounds during the entire campaign is provided in Tables S1–S3. Commonly reported markers for biomass burning in literature include levoglucosan, oxalates, 4-nitrocatechol, monosaccharide anhydrides, and various combustion products.^{26,63} In previous field measurements, sugars, aromatics, organic acids, and terpenoid compounds were reported in $PM_{2.5}$ measured 60 km downwind of wildfire plumes.^{64,65} Levoglucosan, nitro-aromatics, and organic acids were reported from the FIREX-AQ 2019 campaign.²⁵ The aforementioned studies either sampled from an aircraft or less than 100 km from the wildfire emission source. In this study, although levoglucosan was not detected in appreciable amounts, we observed a substantial presence of sugar-like compounds together with highly oxidized organics, including $C_4H_2O_4$, $C_4H_6O_5$, $C_4H_8O_2$, and $C_6H_{12}O_6$. While the exact identity of these compounds remains uncertain, they are consistent with potential natural products and organic acids. These compounds can result from the thermal degradation of plant material and represent products of the continuous oxidation of traditional biomass-burning markers.

Although widely considered a biomass-burning marker, levoglucosan (like other organics) is known to undergo additional oxidation reactions.⁶⁶ Vasilakopoulou *et al.*, (2023) hypothesized that levoglucosan and other traditional biomass-burning markers may undergo rapid atmospheric

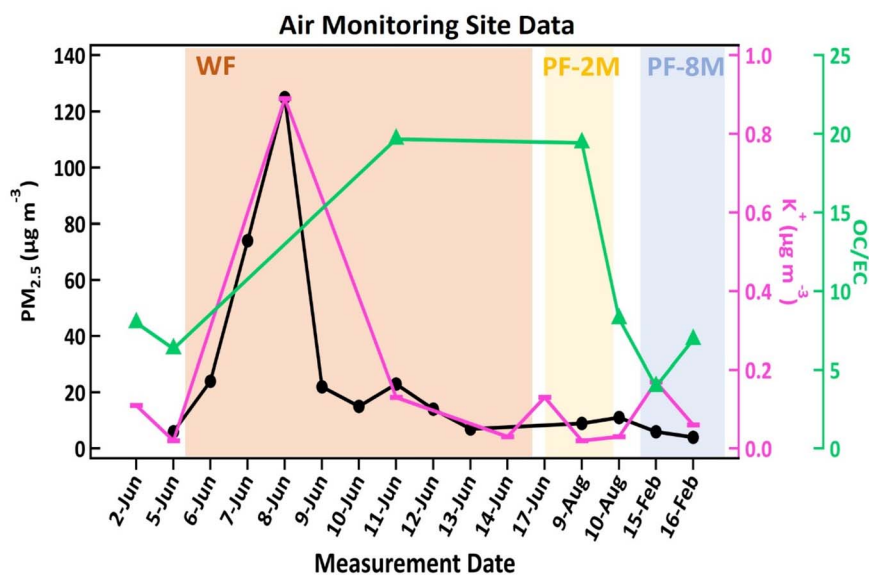


Fig. 7 Observations showing $PM_{2.5}$ (black), K^+ (pink), and OC/EC (green) from the Beltsville Monitoring and EPA Chemical Speciation Network (CSN) site before, during, and after (2 and 8 months post wildfire) the 2023 Canadian wildfire event.



transformations. Other studies have further confirmed the chemical degradation of levoglucosan in the atmosphere, with an atmospheric lifetime of less than 2 days.^{67,68} Additionally, more studies indicate that conventional biomass burning markers are associated with short-range transport from burning emissions, suggesting they are short-lived and susceptible to further physical transformation and/or chemical reactions.⁶⁹ In this work, the particulate emissions observed are from ground-based measurements and have traveled approximately 1700 km (1000 miles) from the source. Hence, levoglucosan is not significantly observed in the composition.

4 Summary and conclusion

Wildfires impact air quality on a regional scale. PM investigated in this study were transported from Canada (~1000 miles) in 2–3 days. The composition of organic aerosol sampled in the Mid-Atlantic had significantly aged and contained water-soluble carbonaceous material. Here, day, night, and extended period (60 hours) samples were extracted from sampling filters and characterized on an LC-MS/MS to determine the abundance of water-soluble organic compounds. It is noted that due to the limitations of instrumentation availability at the site, the absolute contribution of WSOC to the total aerosol composition during this event is unknown. However, the molecular-level speciation of organics in the atmosphere is needed to understand reaction mechanisms and subsequent impacts on regional air quality, climate, and health.

Thus, this work provides additional evidence for speciated water-soluble organic compounds identified from wildfire events. The majority of the reported ions made up the CHO and CHON classes. The presence of CHONP, CHONS, and CHN classes underscores the chemical diversity of nitrogen-containing WSOCs in combustion-derived aerosols: CHONPs, though rare, indicate complex multi-heteroatom chemistry; CHONS species reflect minor yet atmospherically relevant secondary products; and CHN compounds point to direct emissions from biomass pyrolysis and their persistence during long-range transport. The relative distribution of these groups suggests that CHOP compounds, though less common, represent a toxicologically significant fraction; CHOS species illustrate the role of atmospheric processing in adding sulfur functionality; and CHX species highlight halogenated byproducts of coal and waste burning, with minor groups underscoring the overall molecular complexity of combustion-derived aerosols.

This study provides molecular-level information on the composition of observed signals but does not resolve the exact structures or definitive identities of the detected compounds. Instead, we highlight compositional trends within compound groups across the sampling period. Specifically, we report the molecular composition of water-soluble organic compounds (WSOCs) associated with long-range transported wildfire particles. A key limitation is the absence of internal standards, which precludes quantification of absolute concentrations. Nonetheless, the relative abundance of ion signals offers valuable insights into compound distributions and source-related

variability. Furthermore, while our approach enables high-resolution molecular characterization, additional analytical techniques, such as tandem mass spectrometry with authentic standards or complementary spectroscopic methods, would be required to establish unambiguous structural assignments for the ions detected and reported here.

Additionally, information on the chemical composition of particles prevalent during the 2023 East Coast event is rare. To our knowledge, few, if any, studies have reported the molecular-level data of WSOC of particulate wildfire emissions at such a long distance. The range of compounds identified from the non-targeted analysis provides a basis to further explore the diverse range of atmospheric chemistry that can occur in biomass-burning plumes. Eventually, more long-range chemical speciation studies are needed to understand wildfire emissions' influence and predict their impact on tropospheric chemistry. Future studies should also incorporate multi-site and extended sampling for a comprehensive investigation into the spatial variability and long-term changes of wildfire-derived aerosols.

Author contributions

Esther A. Olonimoyo – writing – original draft, data curation, investigation, methodology, formal analysis. Martin Changman Ahn – data curation. Dewansh Rastogi – data curation. Yue Li – mass spectrometer analysis. Candice M. Duncan – funding acquisition, writing – review, supervision, Akua Asa-Awuku – writing – review & editing, supervision, visualization, funding acquisition.

Conflicts of interest

There are no conflicts of interest to declare.

Data availability

The data supporting this article have been included as part of the supplementary information (SI). Supplementary information is available. See DOI: <https://doi.org/10.1039/d5ea00119f>.

Acknowledgements

This research was funded in part by the National Science Foundation [award no. 2051076]. EAO, CMD and AAA would like to thank the NSF for graduate research funding support. In addition, we would like to thank Professor Russell Dickerson (University of Maryland, College Park) and Joel Dreesen (Maryland Department of the Environment) for their assistance and access to additional data sets presented. We also thank Stephanie Jacoby for their assistance in making Fig. 7.

References

- 1 R. Xu, T. Ye, X. Yue, Z. Yang, W. Yu, Y. Zhang, *et al.*, Global population exposure to landscape fire air pollution from



- 2000 to 2019, *Nature*, 2023, **621**(7979), 521–529, DOI: [10.1038/s41586-023-06398-6](https://doi.org/10.1038/s41586-023-06398-6).
- 2 J. M. Roberts, C. E. Stockwell, R. J. Yokelson, J. De Gouw, Y. Liu, V. Selimovic, *et al.*, The nitrogen budget of laboratory-simulated western US wildfires during the FIREX 2016 Fire Lab study, *Atmos. Chem. Phys.*, 2020, **20**, 8807–8826, DOI: [10.5194/ACP-20-8807-2020](https://doi.org/10.5194/ACP-20-8807-2020).
- 3 G. Lai and Y. Zhang, Increased Atmospheric Aridity and Reduced Precipitation Drive the 2023 Extreme Wildfire Season in Canada, *Geophys. Res. Lett.*, 2025, **52**, e2024GL114492, DOI: [10.1029/2024GL114492](https://doi.org/10.1029/2024GL114492).
- 4 *Canada Report 2023 Fire Season*, 2024.
- 5 W. Knorr, F. Dentener, S. Hantson, L. Jiang, Z. Klimont and A. Arneth, Air quality impacts of European wildfire emissions in a changing climate, *Atmos. Chem. Phys.*, 2016, **16**, 5685–5703, DOI: [10.5194/ACP-16-5685-2016](https://doi.org/10.5194/ACP-16-5685-2016).
- 6 G. R. Van Der Werf, J. T. Randerson, L. Giglio, T. T. Van Leeuwen, Y. Chen, B. M. Rogers, *et al.*, Global fire emissions estimates during 1997–2016, *Earth Syst. Sci. Data*, 2017, **9**, 697–720, DOI: [10.5194/ESSD-9-697-2017](https://doi.org/10.5194/ESSD-9-697-2017).
- 7 R. P. Fadadu, G. Solomon and J. R. Balmes, Wildfires and Human Health, *JAMA, J. Am. Med. Assoc.*, 2024, **332**(12), 1011–1012, DOI: [10.1001/JAMA.2024.13600](https://doi.org/10.1001/JAMA.2024.13600).
- 8 Y. Liu, S. Goodrick and W. Heilman, Wildland fire emissions, carbon, and climate: wildfire–climate interactions, *For. Ecol. Manag.*, 2014, **317**, 80–96, DOI: [10.1016/J.FORECO.2013.02.020](https://doi.org/10.1016/J.FORECO.2013.02.020).
- 9 H. M. Rogers, J. C. Ditto and D. R. Gentner, Evidence for impacts on surface-level air quality in the northeastern US from long-distance transport of smoke from North American fires during the Long Island Sound Tropospheric Ozone Study (LISTOS) 2018, *Atmos. Chem. Phys.*, 2020, **20**, 671–682, DOI: [10.5194/ACP-20-671-2020](https://doi.org/10.5194/ACP-20-671-2020).
- 10 R. Farley, N. Bernays, D. A. Jaffe, D. Ketcherside, L. Hu, S. Zhou, *et al.*, Persistent Influence of Wildfire Emissions in the Western United States and Characteristics of Aged Biomass Burning Organic Aerosols under Clean Air Conditions, *Environ. Sci. Technol.*, 2022, **56**, 3645–3657, DOI: [10.1021/ACS.EST.1C07301](https://doi.org/10.1021/ACS.EST.1C07301).
- 11 M. S. Johnson, K. Strawbridge, K. E. Knowland, C. Keller and M. Travis, Long-range transport of Siberian biomass burning emissions to North America during FIREX-AQ, *Atmos. Environ.*, 2021, **252**, 118241, DOI: [10.1016/J.ATMOSENV.2021.118241](https://doi.org/10.1016/J.ATMOSENV.2021.118241).
- 12 L. D. Anderson, B. Dix, J. Schnell, R. Yokelson, J. P. Veefkind, R. Ahmadov, *et al.*, Analyzing the Impact of Evolving Combustion Conditions on the Composition of Wildfire Emissions Using Satellite Data, *Geophys. Res. Lett.*, 2023, **50**, e2023GL105811, DOI: [10.1029/2023GL105811](https://doi.org/10.1029/2023GL105811).
- 13 M. R. Giordano, J. Chong, D. R. Weise and A. A. Asa-Awuku, Does chronic nitrogen deposition during biomass growth affect atmospheric emissions from biomass burning?, *Environ. Res. Lett.*, 2016, **11**, 034007, DOI: [10.1088/1748-9326/11/3/034007](https://doi.org/10.1088/1748-9326/11/3/034007).
- 14 M. J. Gunsch, N. W. May, M. Wen, C. Bottenus, D. J. Gardner, T. M. Vanreken, *et al.*, Ubiquitous influence of wildfire emissions and secondary organic aerosol on summertime atmospheric aerosol in the forested Great Lakes region, *Atmos. Chem. Phys.*, 2018, **18**, 3701–3715, DOI: [10.5194/ACP-18-3701-2018](https://doi.org/10.5194/ACP-18-3701-2018).
- 15 Y. Liu, S. L. Goodrick and J. A. Stanturf, Future U.S. wildfire potential trends projected using a dynamically downscaled climate change scenario, *For. Ecol. Manag.*, 2013, **294**, 120–135, DOI: [10.1016/J.FORECO.2012.06.049](https://doi.org/10.1016/J.FORECO.2012.06.049).
- 16 Y. Sun, Q. Zhang, Z. Qin, K. Li and Y. Zhang, Laboratory study on the characteristics of fresh and aged PM1 emitted from typical forest vegetation combustion in Southwest China, *Environ. Pollut.*, 2024, **359**, 124505, DOI: [10.1016/j.envpol.2024.124505](https://doi.org/10.1016/j.envpol.2024.124505).
- 17 X. Shi, J. Zhang, X. Zhou, Z. Cao, Y. Luo and W. Wang, Wintertime characteristics of water-soluble organic carbon in PM2.5 during haze and non-haze days in Jinan in the North China Plain, *Atmos. Environ.*, 2023, **310**, 119985, DOI: [10.1016/J.ATMOSENV.2023.119985](https://doi.org/10.1016/J.ATMOSENV.2023.119985).
- 18 L. Ma, P. T. M. Tran and R. Balasubramanian, Insight into the abundance and optical characteristics of water-soluble organic compounds (WSOC) in PM2.5 in urban areas, *Chemosphere*, 2025, **372**, 144103, DOI: [10.1016/J.CHEMOSPHERE.2025.144103](https://doi.org/10.1016/J.CHEMOSPHERE.2025.144103).
- 19 S. Lv, C. Wu, F. Wang, X. Liu, S. Zhang, Y. Chen, *et al.*, Nitrate-Enhanced Gas-to-Particle-Phase Partitioning of Water-Soluble Organic Compounds in Chinese Urban Atmosphere: Implications for Secondary Organic Aerosol Formation, *Environ. Sci. Technol. Lett.*, 2023, **10**, 14–20, DOI: [10.1021/ACS.ESTLETT.2C00894](https://doi.org/10.1021/ACS.ESTLETT.2C00894).
- 20 T. Gautam, G. W. Vandergrift, N. N. Lata, Z. Cheng, A. Rahman and A. Minke, Chemical Insights into the Molecular Composition of Organic Aerosols in the Urban Region of Houston, Texas, *ACS ES&T Air*, 2024, **1**(10), 1304–1316, DOI: [10.1021/ACSESTAIR.4C00141](https://doi.org/10.1021/ACSESTAIR.4C00141).
- 21 C. Wang, W. Zhu, Z. Shi and J. Li, A Sensitive Online SPE-LC-APCI-MS/MS Method for Simultaneous Determination of 17 Nitrated and Oxygenated Polycyclic Aromatic Hydrocarbons in Atmospheric Particulate Matter, *Chromatographia*, 2023, **86**, 677–688, DOI: [10.1007/S10337-023-04280-1](https://doi.org/10.1007/S10337-023-04280-1).
- 22 X. Zhang, Z. Liu, A. Hecobian, M. Zheng, N. H. Frank, E. S. Edgerton, *et al.*, Spatial and seasonal variations of fine particle water-soluble organic carbon (WSOC) over the southeastern United States: implications for secondary organic aerosol formation, *Atmos. Chem. Phys.*, 2012, **12**, 6593–6607, DOI: [10.5194/ACP-12-6593-2012](https://doi.org/10.5194/ACP-12-6593-2012).
- 23 R. J. Yokelson, J. D. Crounse, P. F. Decarlo, T. Karl, S. Urbanski, E. Atlas, *et al.*, Emissions from biomass burning in the Yucatan, *Atmos. Chem. Phys.*, 2009, **9**, 5785–5812.
- 24 T. T. H. Mai and H. Kim, Determination of Gaseous and Particulate Secondary Amines in the Atmosphere Using Gas Chromatography Coupled with Electron Capture Detection, *Atmosphere*, 2022, **13**, 664, DOI: [10.3390/ATMOS13050664](https://doi.org/10.3390/ATMOS13050664).
- 25 D. Pagonis, P. Campuzano-Jost, H. Guo, D. A. Day, M. K. Schueneman, W. L. Brown, *et al.*, Airborne extractive electrospray mass spectrometry measurements of the chemical composition of organic aerosol, *Atmos. Meas. Tech.*, 2021, **14**, 1545–1559, DOI: [10.5194/AMT-14-1545-2021](https://doi.org/10.5194/AMT-14-1545-2021).



- 26 A. Yazdani, S. Takahama, J. K. Kodros, M. Paglione, M. Masiol, S. Squizzato, *et al.*, Chemical evolution of primary and secondary biomass burning aerosols during daytime and nighttime, *Atmos. Chem. Phys.*, 2023, **23**, 7461–7477, DOI: [10.5194/ACP-23-7461-2023](https://doi.org/10.5194/ACP-23-7461-2023).
- 27 W. Hu, M. Hu, W. Hu, J. L. Jimenez, B. Yuan, W. Chen, *et al.*, Chemical composition, sources, and aging process of submicron aerosols in Beijing: contrast between summer and winter, *J. Geophys. Res.: Atmos.*, 2016, **121**, 1955–1977, DOI: [10.1002/2015JD024020](https://doi.org/10.1002/2015JD024020).
- 28 S. Samy, J. Robinson and M. D. Hays, An advanced LC-MS (Q-TOF) technique for the detection of amino acids in atmospheric aerosols, *Anal. Bioanal. Chem.*, 2011, **401**, 3103–3113, DOI: [10.1007/S00216-011-5238-2](https://doi.org/10.1007/S00216-011-5238-2).
- 29 E. A. Stone, L. Yang, L. E. Yu and M. Rupakheti, Characterization of organosulfates in atmospheric aerosols at Four Asian locations, *Atmos. Environ.*, 2012, **47**, 323–329, DOI: [10.1016/J.ATMOSENV.2011.10.058](https://doi.org/10.1016/J.ATMOSENV.2011.10.058).
- 30 Y. Ma, X. Xu, W. Song, F. Geng and L. Wang, Seasonal and diurnal variations of particulate organosulfates in urban Shanghai, China, *Atmos. Environ.*, 2014, **85**, 152–160, DOI: [10.1016/J.ATMOSENV.2013.12.017](https://doi.org/10.1016/J.ATMOSENV.2013.12.017).
- 31 B. Jia, K. Zhu, Z. Bai, A. Abudula, B. Liu, J. Yan, *et al.*, Non targeted and targeted LC-MS/MS insights into the composition and concentration of atmospheric microplastics and additives: impacts and regional changes of sandstorms in Shanghai and Hohhot, China, *Sci. Total Environ.*, 2024, **953**, 176254, DOI: [10.1016/J.SCITOTENV.2024.176254](https://doi.org/10.1016/J.SCITOTENV.2024.176254).
- 32 J. Ma, F. Ungeheuer, F. Zheng, W. Du, Y. Wang, J. Cai, *et al.*, Nontarget Screening Exhibits a Seasonal Cycle of PM_{2.5} Organic Aerosol Composition in Beijing, *Environ. Sci. Technol.*, 2022, **56**, 7017–7028, DOI: [10.1021/ACS.EST.1C06905](https://doi.org/10.1021/ACS.EST.1C06905).
- 33 X. Zhang, A. Saini, C. Hao and T. Harner, Passive air sampling and nontargeted analysis for screening POP-like chemicals in the atmosphere: opportunities and challenges, *TrAC, Trends Anal. Chem.*, 2020, **132**, 116052, DOI: [10.1016/J.TRAC.2020.116052](https://doi.org/10.1016/J.TRAC.2020.116052).
- 34 B. Byrne, J. Liu, K. W. Bowman, M. Pascolini-Campbell, A. Chatterjee, S. Pandey, *et al.*, Carbon emissions from the 2023 Canadian wildfires, *Nature*, 2024, **633**, 835–839, DOI: [10.1038/s41586-024-07878-z](https://doi.org/10.1038/s41586-024-07878-z).
- 35 P. Jain, Q. E. Barber, S. W. Taylor, E. Whitman, D. C. Acuna, Y. Boulanger, *et al.*, Drivers and Impacts of the Record-Breaking 2023 Wildfire Season in Canada, *Nat. Commun.*, 2024, **15**(1), 1–14, DOI: [10.1038/s41467-024-51154-7](https://doi.org/10.1038/s41467-024-51154-7).
- 36 M. Yu, S. Zhang, H. Ning, Z. Li and K. Zhang, Assessing the 2023 Canadian wildfire smoke impact in Northeastern US: air quality, exposure and environmental justice, *Sci. Total Environ.*, 2024, **926**, 171853, DOI: [10.1016/J.SCITOTENV.2024.171853](https://doi.org/10.1016/J.SCITOTENV.2024.171853).
- 37 H. Chen, W. Zhang and L. Sheng, Canadian record-breaking wildfires in 2023 and their impact on US air quality, *Atmos. Environ.*, 2025, **342**, 120941, DOI: [10.1016/J.ATMOSENV.2024.120941](https://doi.org/10.1016/J.ATMOSENV.2024.120941).
- 38 X. Sun, Y. Wang, H. Li, X. Yang, L. Sun, X. Wang, *et al.*, Organic acids in cloud water and rainwater at a mountain site in acid rain areas of South China, *Environ. Sci. Pollut. Res.*, 2016, **23**, 9529–9539, DOI: [10.1007/S11356-016-6038-1](https://doi.org/10.1007/S11356-016-6038-1).
- 39 M. R. Canagaratna, J. L. Jimenez, J. H. Kroll, Q. Chen, S. H. Kessler, P. Massoli, *et al.*, Elemental ratio measurements of organic compounds using aerosol mass spectrometry: characterization, improved calibration, and implications, *Atmos. Chem. Phys.*, 2015, **15**, 253–272, DOI: [10.5194/ACP-15-253-2015](https://doi.org/10.5194/ACP-15-253-2015).
- 40 A. F. Stein, R. R. Draxler, G. D. Rolph, B. J. B. Stunder, M. D. Cohen and F. Ngan, NOAA's HYSPLIT atmospheric transport and dispersion modeling system, *Bull. Am. Meteorol. Soc.*, 2015, **96**, 2059–2077, DOI: [10.1175/BAMS-D-14-00110.1](https://doi.org/10.1175/BAMS-D-14-00110.1).
- 41 K. Baldwin, K. Chapman, D. Meidinger, P. Uhlig, L. Allen and S. Basquill, *et al.*, The Canadian National Vegetation Classification: Principles, Methods and Status, *Natural Resources Canada, Canadian Forest Service Information Report GLC-X-23*, 2019.
- 42 M. Xie, X. Chen, M. D. Hays and A. L. Holder, Composition and light absorption of N-containing aromatic compounds in organic aerosols from laboratory biomass burning, *Atmos. Chem. Phys.*, 2019, **19**, 2899–2915, DOI: [10.5194/ACP-19-2899-2019](https://doi.org/10.5194/ACP-19-2899-2019).
- 43 A. Ijaz, W. Kew, S. China, S. K. Schum and L. R. Mazzoleni, Molecular Characterization of Organophosphorus Compounds in Wildfire Smoke Using 21-T Fourier Transform-Ion Cyclotron Resonance Mass Spectrometry, *Anal. Chem.*, 2022, **94**, 14537–14545, DOI: [10.1021/ACS.ANALCHEM.2C00916](https://doi.org/10.1021/ACS.ANALCHEM.2C00916).
- 44 J. C. Ditto, M. He, T. N. Hass-Mitchell, S. G. Moussa, K. Hayden, S. M. Li, *et al.*, Atmospheric evolution of emissions from a boreal forest fire: the formation of highly functionalized oxygen-, nitrogen-, and sulfur-containing organic compounds, *Atmos. Chem. Phys.*, 2021, **21**, 255–267, DOI: [10.5194/ACP-21-255-2021](https://doi.org/10.5194/ACP-21-255-2021).
- 45 T. Nakamura, H. Ogawa, D. K. Maripi and M. Uematsu, Contribution of water soluble organic nitrogen to total nitrogen in marine aerosols over the East China Sea and western North Pacific, *Atmos. Environ.*, 2006, **40**, 7259–7264, DOI: [10.1016/J.ATMOSENV.2006.06.026](https://doi.org/10.1016/J.ATMOSENV.2006.06.026).
- 46 A. Laskin, J. S. Smith and J. Laskin, Molecular characterization of nitrogen-containing organic compounds in biomass burning aerosols using high-resolution mass spectrometry, *Environ. Sci. Technol.*, 2009, **43**, 3764–3771, DOI: [10.1021/ES803456N](https://doi.org/10.1021/ES803456N).
- 47 B. H. Lee, C. Mohr, F. D. Lopez-Hilfiker, A. Lutz, M. Hallquist, L. Lee, *et al.*, Highly functionalized organic nitrates in the southeast United States: contribution to secondary organic aerosol and reactive nitrogen budgets, *Proc. Natl. Acad. Sci. U. S. A.*, 2016, **113**, 1516–1521, DOI: [10.1073/PNAS.1508108113](https://doi.org/10.1073/PNAS.1508108113).
- 48 H. Mali, C. Shah, B. H. Raghunandan, A. S. Prajapati, D. H. Patel, U. Trivedi, *et al.*, Organophosphate pesticides an emerging environmental contaminant: pollution, toxicity, bioremediation progress, and remaining



- challenges, *J. Environ. Sci.*, 2023, **127**, 234–250, DOI: [10.1016/J.JES.2022.04.023](https://doi.org/10.1016/J.JES.2022.04.023).
- 49 M. Kanakidou, S. Myriokefalitakis and K. Tsigaridis, Aerosols in atmospheric chemistry and biogeochemical cycles of nutrients, *Environ. Res. Lett.*, 2018, **13**, 063004, DOI: [10.1088/1748-9326/AABCDB](https://doi.org/10.1088/1748-9326/AABCDB).
- 50 S. Myriokefalitakis, A. Nenes, A. R. Baker, N. Mihalopoulos and M. Kanakidou, Bioavailable atmospheric phosphorous supply to the global ocean: a 3-D global modeling study, *Biogeosciences*, 2016, **13**, 6519–6543, DOI: [10.5194/BG-13-6519-2016](https://doi.org/10.5194/BG-13-6519-2016).
- 51 R. Jin, G. Liu, X. Jiang, Y. Liang, H. Fiedler, L. Yang, *et al.*, Profiles, sources and potential exposures of parent, chlorinated and brominated polycyclic aromatic hydrocarbons in haze associated atmosphere, *Sci. Total Environ.*, 2017, **593–594**, 390–398, DOI: [10.1016/J.SCITOTENV.2017.03.134](https://doi.org/10.1016/J.SCITOTENV.2017.03.134).
- 52 H. Zhang, Y. Ji, Z. Wu, L. Peng, J. Bao, Z. Peng, *et al.*, Atmospheric volatile halogenated hydrocarbons in air pollution episodes in an urban area of Beijing: characterization, health risk assessment and sources apportionment, *Sci. Total Environ.*, 2022, **806**, 150283, DOI: [10.1016/J.SCITOTENV.2021.150283](https://doi.org/10.1016/J.SCITOTENV.2021.150283).
- 53 H. Guo, A. J. Ding, T. Wang, I. J. Simpson, D. R. Blake and B. Barletta, Source origins, modeled profiles, and apportionments of halogenated hydrocarbons in the greater Pearl River Delta region, southern China, *J. Geophys. Res.:Atmos.*, 2009, **114**, 1–19, DOI: [10.1029/2008JD011448](https://doi.org/10.1029/2008JD011448).
- 54 K. Kawamura and K. Ikushima, Seasonal Changes in the Distribution of Dicarboxylic Acids in the Urban Atmosphere, *Environ. Sci. Technol.*, 1993, **27**, 2227–2235.
- 55 P. Q. Fu, K. Kawamura, C. M. Pavuluri, T. Swaminathan and J. Chen, Molecular characterization of urban organic aerosol in tropical India: Contributions of primary emissions and secondary photooxidation, *Atmos. Chem. Phys.*, 2010, **10**, 2663–2689, DOI: [10.5194/ACP-10-2663-2010](https://doi.org/10.5194/ACP-10-2663-2010).
- 56 J. Brito, L. V. Rizzo, W. T. Morgan, H. Coe, B. Johnson, J. Haywood, *et al.*, Ground-based aerosol characterization during the South American Biomass Burning Analysis (SAMBBA) field experiment, *Atmos. Chem. Phys.*, 2014, **14**, 12069–12083, DOI: [10.5194/ACP-14-12069-2014](https://doi.org/10.5194/ACP-14-12069-2014).
- 57 S. Zhou, S. Collier, D. A. Jaffe, N. L. Briggs, J. Hee, A. J. S. Iii, *et al.*, Regional influence of wildfires on aerosol chemistry in the western US and insights into atmospheric aging of biomass burning organic aerosol, *Atmos. Chem. Phys.*, 2017, **17**, 2477–2493, DOI: [10.5194/ACP-17-2477-2017](https://doi.org/10.5194/ACP-17-2477-2017).
- 58 Q. Chen, D. K. Farmer, J. Schneider, S. R. Zorn, C. L. Heald and T. G. Karl, Mass spectral characterization of submicron biogenic organic particles in the Amazon Basin, *Geophys. Res. Lett.*, 2009, **36**(20), 1–5, DOI: [10.1029/2009GL039880](https://doi.org/10.1029/2009GL039880).
- 59 S. Gilardoni, P. Massoli, M. Paglione, L. Giulianelli, C. Carbone, M. Rinaldi, *et al.*, Direct observation of aqueous secondary organic aerosol from biomass-burning emissions, *Proc. Natl. Acad. Sci. U. S. A.*, 2016, **113**, 10013–10018, DOI: [10.1073/PNAS.1602212113](https://doi.org/10.1073/PNAS.1602212113).
- 60 Z. C. J. Decker, M. A. Robinson, K. C. Barsanti, I. Bourgeois, M. M. Coggon, J. P. Digangi, *et al.*, Nighttime and daytime dark oxidation chemistry in wildfire plumes: an observation and model analysis of FIREX-AQ aircraft data, *Atmos. Chem. Phys.*, 2021, **21**, 16293–16317, DOI: [10.5194/ACP-21-16293-2021](https://doi.org/10.5194/ACP-21-16293-2021).
- 61 J. Y. Lee, P. K. Peterson, L. R. Vear, R. D. Cook, A. P. Sullivan, E. Smith, *et al.*, Wildfire Smoke Influence on Cloud Water Chemical Composition at Whiteface Mountain, New York, *J. Geophys. Res.:Atmos.*, 2022, **127**, e2022JD037177, DOI: [10.1029/2022JD037177](https://doi.org/10.1029/2022JD037177).
- 62 A. P. Sullivan, H. Guo, J. C. Schroder, P. Campuzano-Jost, J. L. Jimenez, T. Campos, *et al.*, Biomass Burning Markers and Residential Burning in the WINTER Aircraft Campaign, *J. Geophys. Res.:Atmos.*, 2019, **124**, 1846–1861, DOI: [10.1029/2017JD028153](https://doi.org/10.1029/2017JD028153).
- 63 H. Bhattarai, E. Saikawa, X. Wan, H. Zhu, K. Ram, S. Gao, *et al.*, Levoglucosan as a tracer of biomass burning: recent progress and perspectives, *Atmos. Res.*, 2019, **220**, 20–33, DOI: [10.1016/J.ATMOSRES.2019.01.004](https://doi.org/10.1016/J.ATMOSRES.2019.01.004).
- 64 Y. Liang, C. N. Jen, R. J. Weber, P. K. Misztal and A. H. Goldstein, Chemical composition of PM_{2.5} in October 2017 Northern California wildfire plumes, *Atmos. Chem. Phys.*, 2021, **21**, 5719–5737, DOI: [10.5194/ACP-21-5719-2021](https://doi.org/10.5194/ACP-21-5719-2021).
- 65 Y. Liang, C. Stamatis, E. C. Fortner, R. A. Wernis, P. Van Rooy, F. Majluf, *et al.*, Emissions of organic compounds from western US wildfires and their near-fire transformations, *Atmos. Chem. Phys.*, 2022, **22**, 9877–9893, DOI: [10.5194/acp-22-9877-2022](https://doi.org/10.5194/acp-22-9877-2022).
- 66 C. N. Vasilakopoulou, A. Matrali, K. Skyllakou, M. Georgopoulou, A. Aktypis, K. Florou, *et al.*, Rapid transformation of wildfire emissions to harmful background aerosol, *npj Clim. Atmos. Sci.*, 2023, **6**(1), 1–9, DOI: [10.1038/s41612-023-00544-7](https://doi.org/10.1038/s41612-023-00544-7).
- 67 Y. Hong, F. Cao, M. Y. Fan, Y. C. Lin, C. Gul, M. Yu, *et al.*, Impacts of chemical degradation of levoglucosan on quantifying biomass burning contribution to carbonaceous aerosols: a case study in Northeast China, *Sci. Total Environ.*, 2022, **819**, 152007, DOI: [10.1016/J.SCITOTENV.2021.152007](https://doi.org/10.1016/J.SCITOTENV.2021.152007).
- 68 Y. Li, T. M. Fu, J. Z. Yu, X. Feng, L. Zhang, J. Chen, *et al.*, Impacts of Chemical Degradation on the Global Budget of Atmospheric Levoglucosan and Its Use As a Biomass Burning Tracer, *Environ. Sci. Technol.*, 2021, **55**, 5525–5536, DOI: [10.1021/ACS.EST.0C07313](https://doi.org/10.1021/ACS.EST.0C07313).
- 69 J. Zhang, A. Zuend, J. Top, M. Surdu, I. E. Haddad, J. G. Slowik, *et al.*, Estimation of the Volatility and Apparent Activity Coefficient of Levoglucosan in Wood-Burning Organic Aerosols, *Environ. Sci. Technol. Lett.*, 2024, **11**, 1214–1219, DOI: [10.1021/ACS.ESTLETT.4C00608](https://doi.org/10.1021/ACS.ESTLETT.4C00608).

